SUPPORTING INFORMATION

Deconvoluting the Molecular Control of Binding and Signaling at the Amylin 3 (AMY_3) Receptor: RAMP3 Alters Signal Propagation Through Extracellular Loops of the Calcitonin Receptor

Vi Pham[1#], Yue Zhu[2,3#], Emma Dal Maso[1#], Christopher A. Reynolds[4], Giuseppe Deganutti[4], Silvia Atanasio[4], Caroline A. Hick[1], Dehua Yang[2], Arthur Christopoulos[1], Debbie L. Hay[5], Sebastian G.B. Furness[1], Ming-Wei Wang[2,3*], Denise Wootten[1*], Patrick M. Sexton[1*]

[1]Drug Discovery Biology, Monash Institute of Pharmaceutical Sciences, Monash University, Parkville 3052, Victoria, Australia
[2]The National Center for Drug Screening and CAS Key Laboratory of Receptor Research, Shanghai Institute of Materia Medica, Chinese Academy of Sciences, Shanghai 201203
[3]University of Chinese Academy of Sciences, 19A Yuquan Road, Beijing 100049, China
[4]School of Biological Sciences, University of Essex, Wivenhoe Park, Colchester CO4 3SQ, UK
[5]The University of Auckland, School of Biological Sciences, 3 Symonds Street, Auckland 1142, New Zealand

[#]These authors contributed equally to this work.

***Address correspondence to:**
Patrick M. Sexton (Patrick.sexton@monash.edu) or
Denise Wootten (denise.wootten@monash.edu) or
Ming-Wei Wang (mwwang@simm.ac.cn)

Supplementary Figures 1 - 16

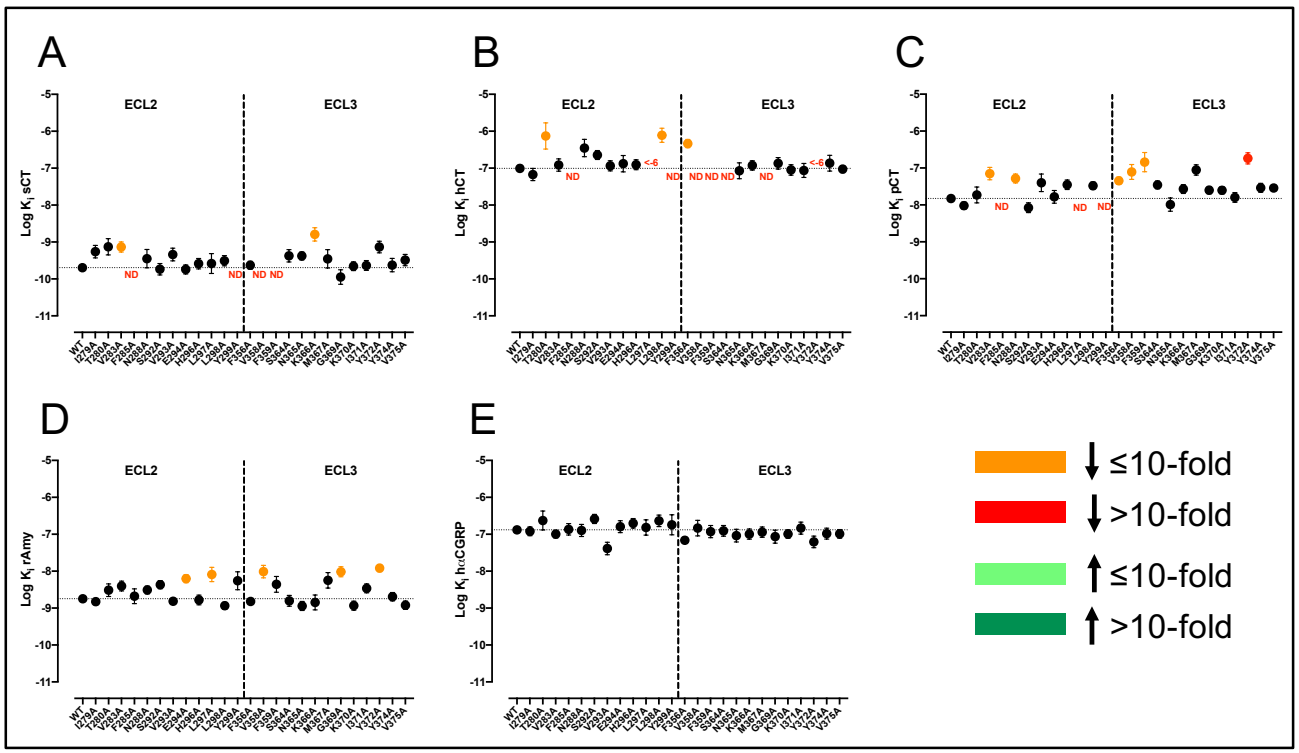

Figure S1. Alanine mutation of ECL2 and ECL3 of AMY_3R selectively alters peptide affinity. For each receptor mutant and ligand, competition binding curves were established using 125I-rAmy as radioligand and log K_i determined: (A) effect of ECL mutants on sCT log K_i; (B) effect of ECL mutants on hCT log K_i; (C) effect of ECL mutants on pCT log K_i; (D) effect of ECL mutants on rAmy log K_i; (E) effect of ECL mutants on hCGRP log K_i. Significance of changes was established by comparison of the WT to the other receptor mutants in a one-way ANOVA and Dunnett's post-test to determine log K_i values with significant changes ($P < 0.05$) denoted by coloured symbols; dark orange, ≤10-fold decrease; red, >10-fold decrease). N.D., affinity not determined. The dotted line is the WT mean.

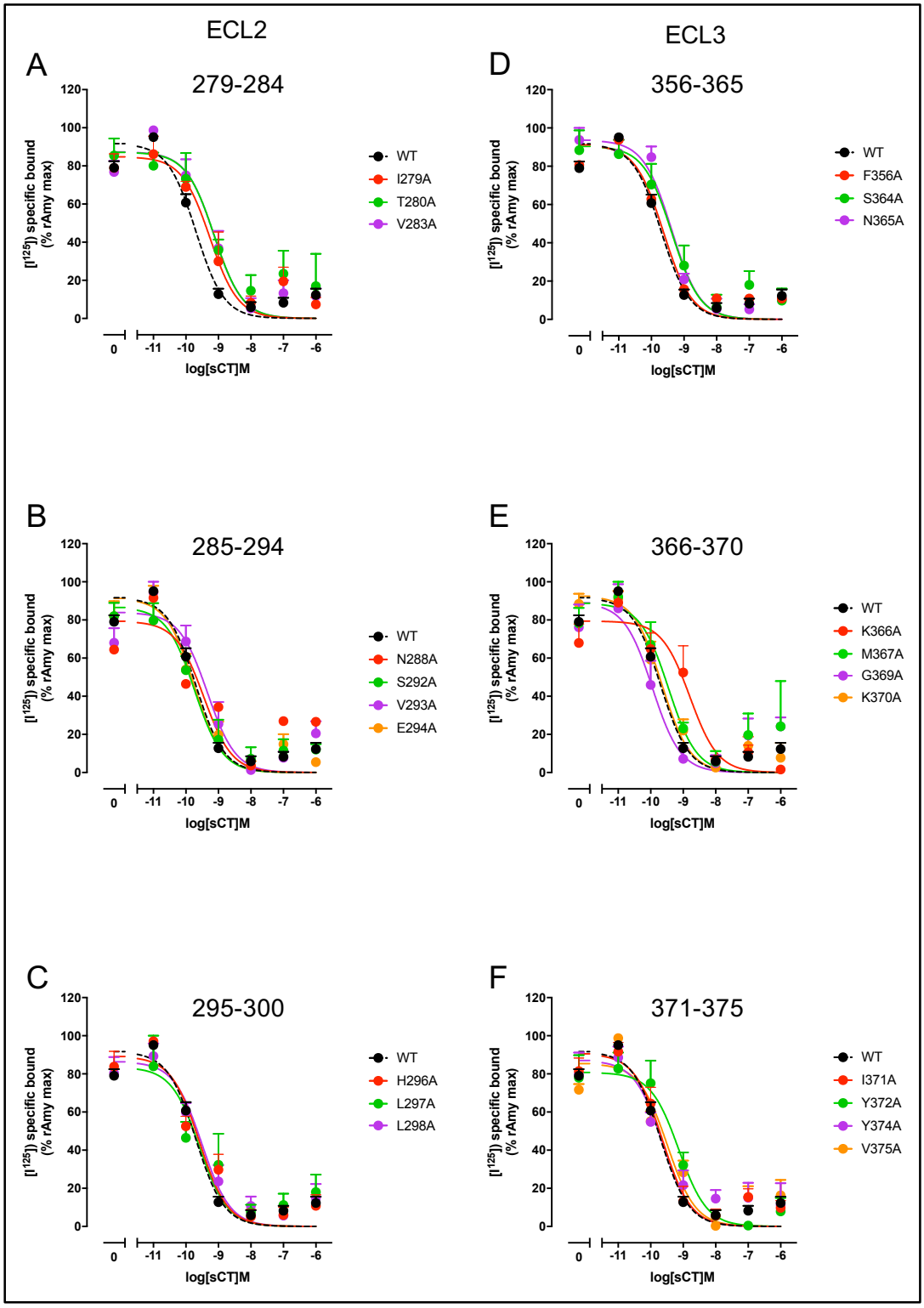

Figure S2. Competition binding isotherms for sCT in competition for 125I-rAmy at the WT and mutant AMY_3R. **A-C.** Mutations of ECL2. **D-F.** Mutations of ECL3. Data have been normalized to the total binding for each receptor mutant (or wild-type) from homologous competition (100%) and non-specific binding, defined by 1 µM rAmy, has been subtracted (giving % specific binding). Data have been fit with a 3-parameter logistic equation. Data are mean + SEM from 3-16 independent experiments (specific "n" numbers are shown in Table 1).

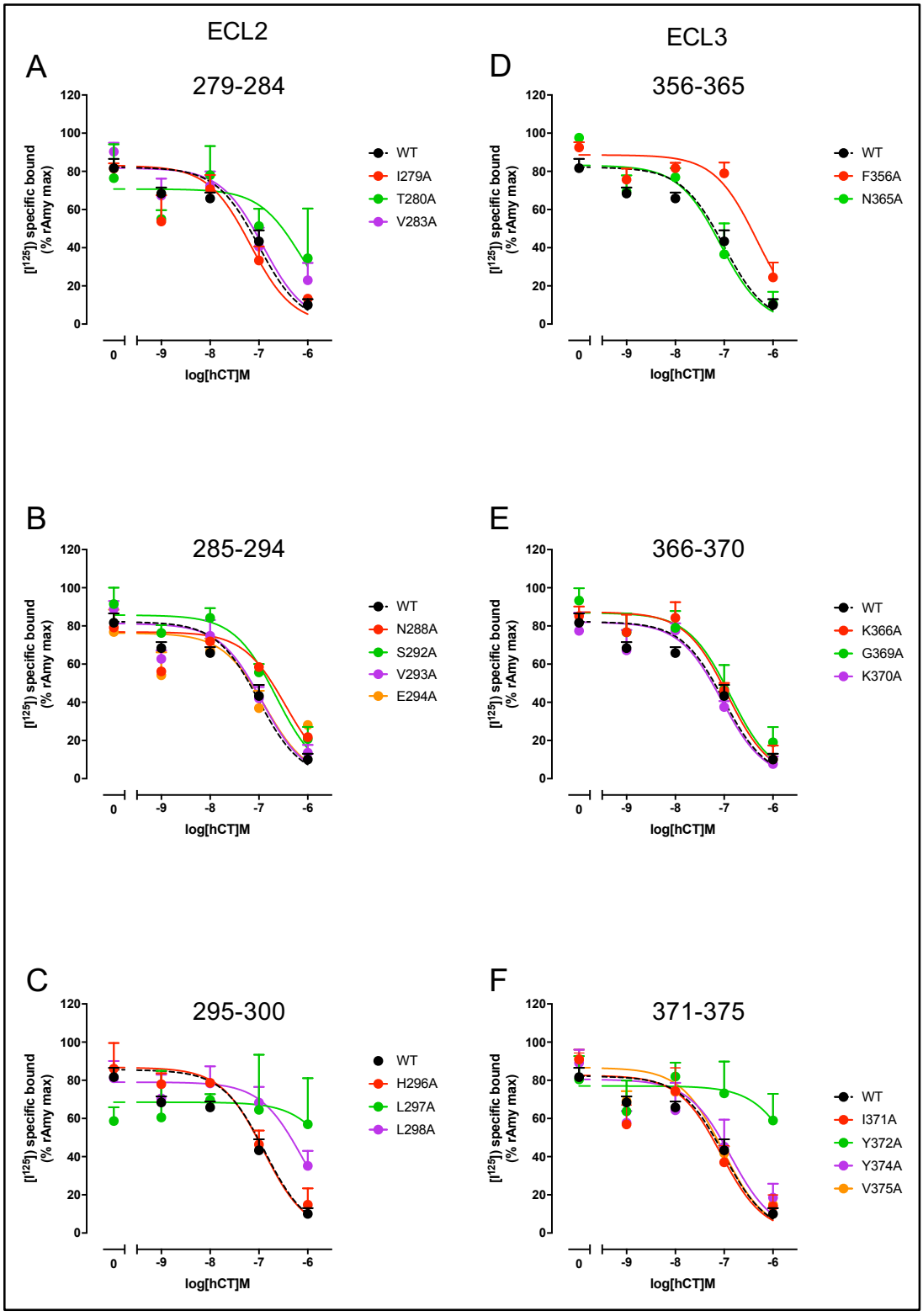

Figure S3. Competition binding isotherms for hCT in competition for 125I-rAmy at the WT and mutant AMY_3R. **A-C.** Mutations of ECL2. **D-F.** Mutations of ECL3. Data have been normalized to the total binding for each receptor mutant (or wild-type) from homologous competition (100%) and non-specific binding, defined by 1 µM rAmy, has been subtracted (giving % specific binding). Data have been fit with a 3-parameter logistic equation. Data are mean + SEM from 3-17 independent experiments (specific "n" numbers are shown in Table 1).

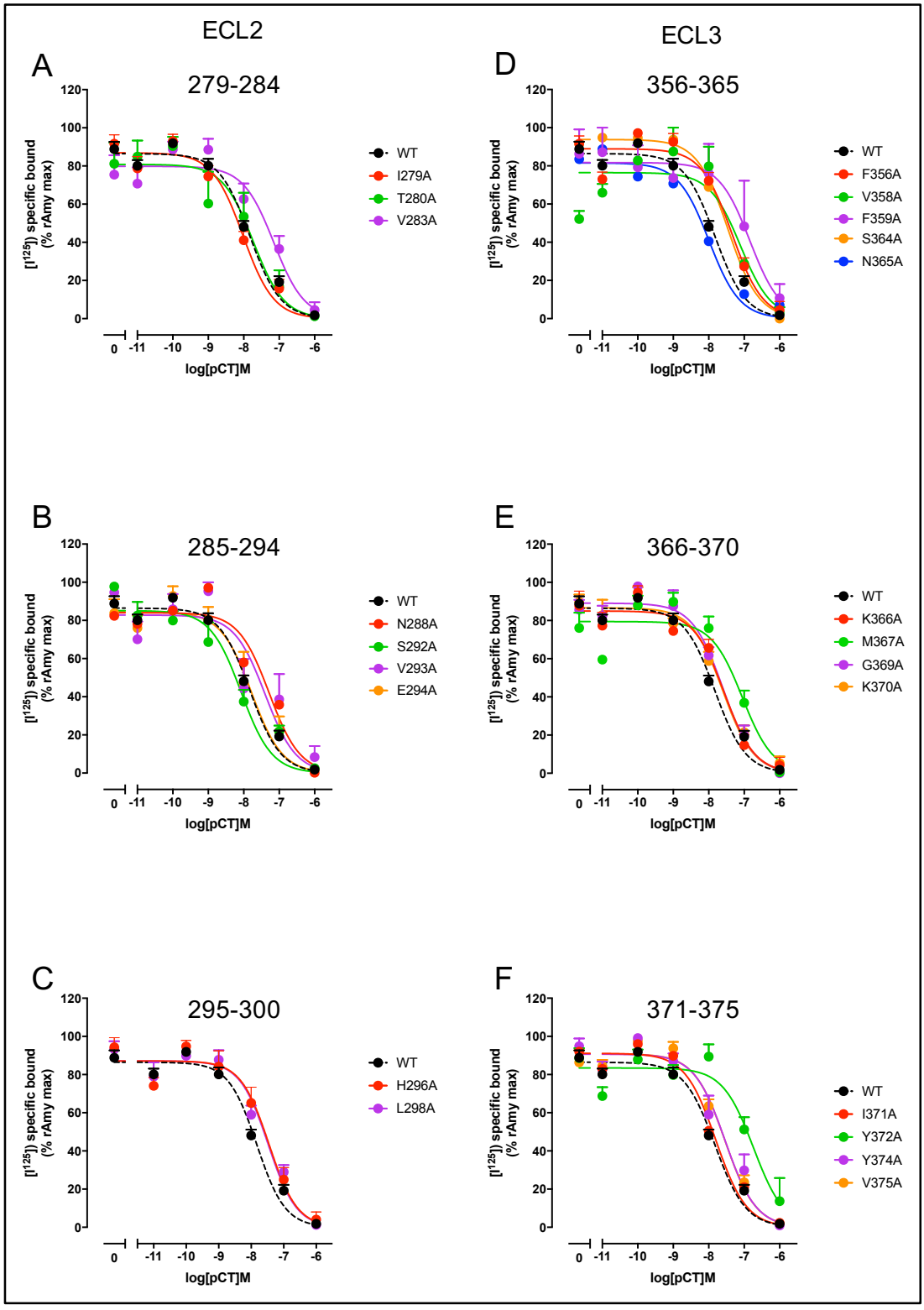

Figure S4. Competition binding isotherms for pCT in competition for 125I-rAmy at the WT and mutant AMY_3R. **A-C.** Mutations of ECL2. **D-F.** Mutations of ECL3. Data have been normalized to the total binding for each receptor mutant (or wild-type) from homologous competition (100%) and non-specific binding, defined by 1 µM rAmy, has been subtracted (giving % specific binding). Data have been fit with a 3-parameter logistic equation. Data are mean + SEM from 3-17 independent experiments (specific "n" numbers are shown in Table 1).

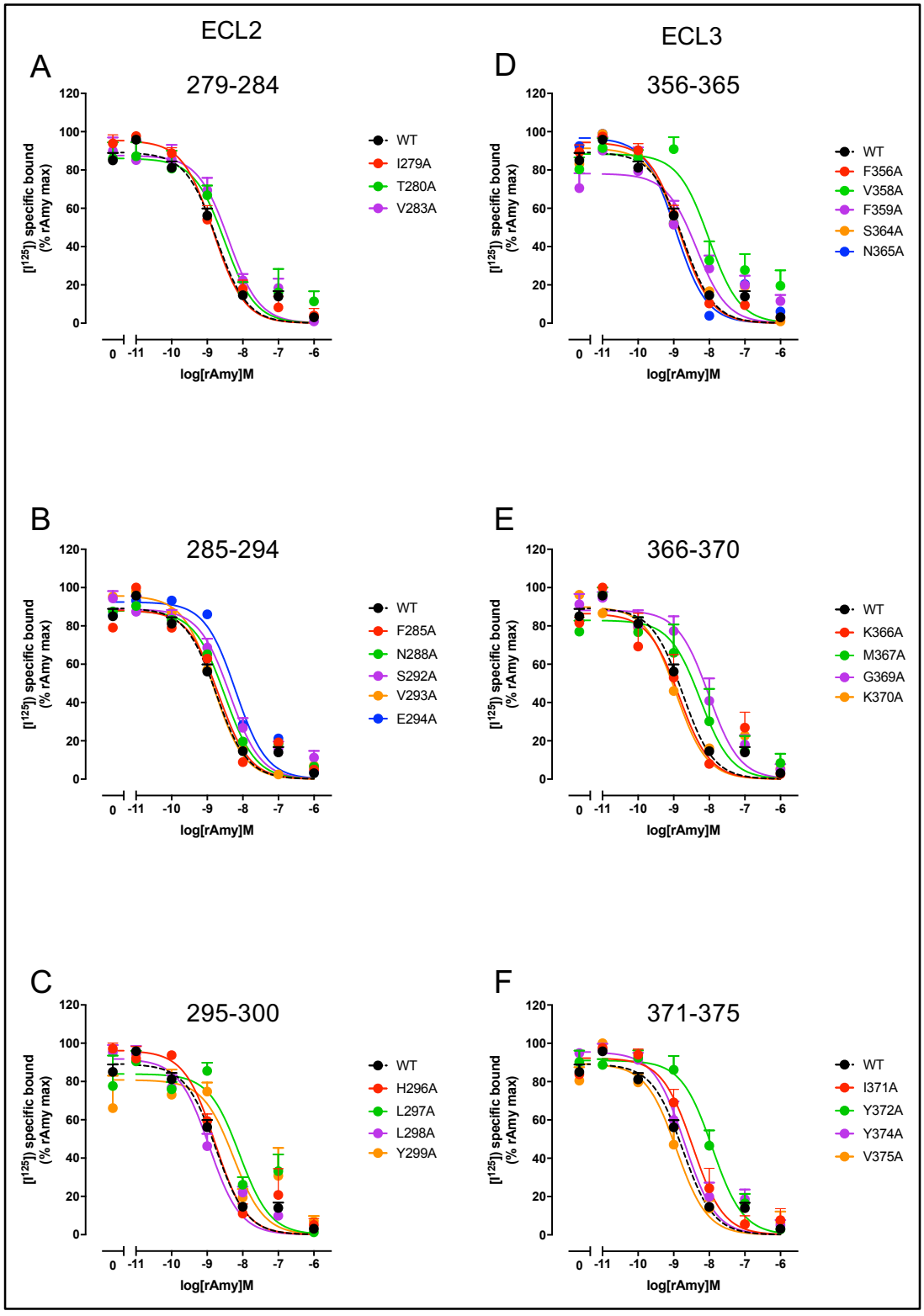

Figure S5. Competition binding isotherms for rAmy in competition for 125I-rAmy at the WT and mutant AMY_3R. **A-C.** Mutations of ECL2. **D-F.** Mutations of ECL3. Data have been normalized to the total binding for each receptor mutant (or wild-type) from homologous competition (100%) and non-specific binding, defined by 1 µM rAmy, has been subtracted (giving % specific binding). Data have been fit with a 3-parameter logistic equation. Data are mean + SEM from 3-19 independent experiments (specific "n" numbers are shown in Table 1).

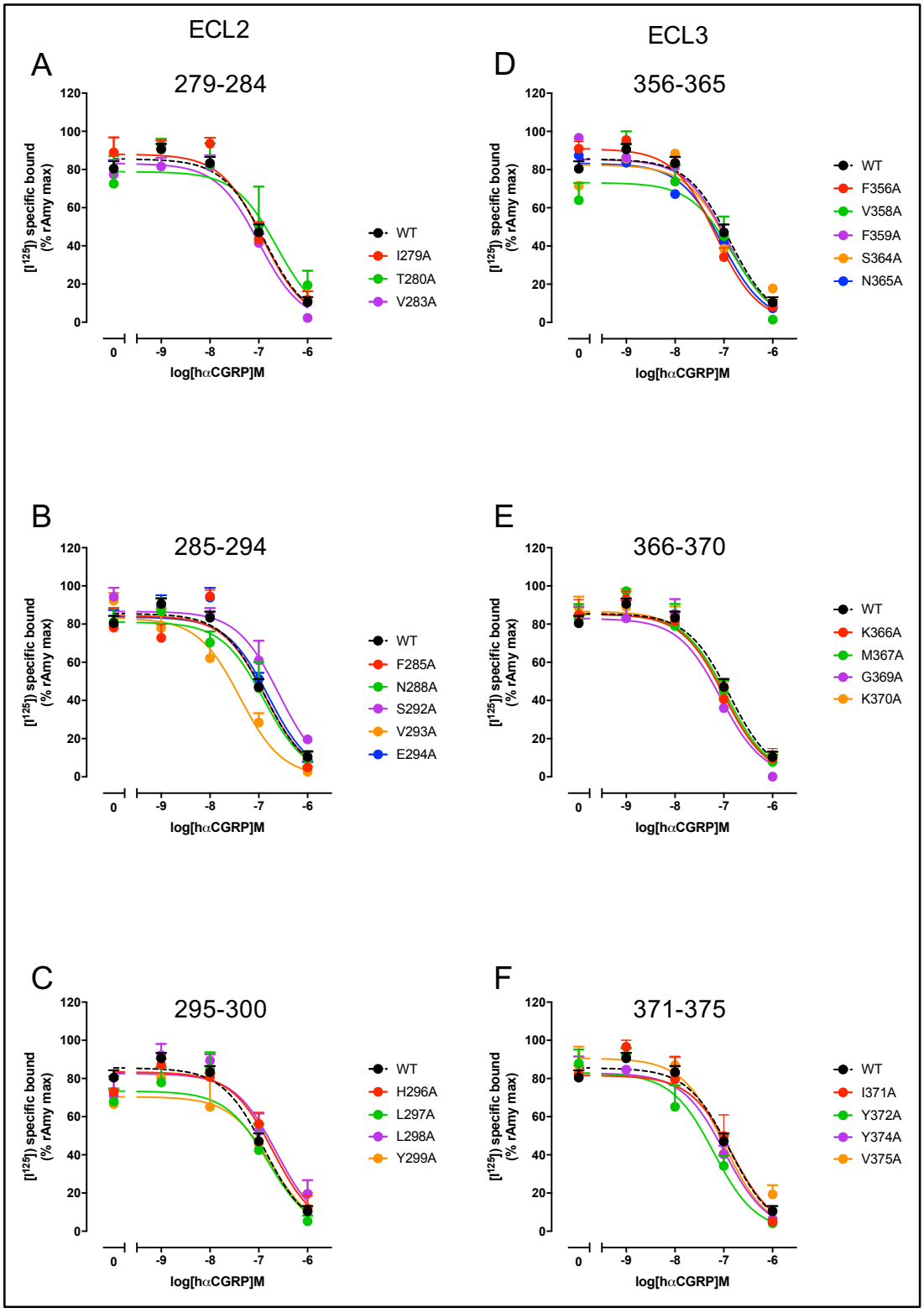

Figure S6. Competition binding isotherms for hCGRP in competition for 125I-rAmy at the WT and mutant AMY_3R. **A-C.** Mutations of ECL2. **D-F.** Mutations of ECL3. Data have been normalized to the total binding for each receptor mutant (or wild-type) from homologous competition (100%) and non-specific binding, defined by 1 µM rAmy, has been subtracted (giving % specific binding). Data have been fit with a 3-parameter logistic equation. Data are mean + SEM from 3-17 independent experiments (specific "n" numbers are shown in Table 1).

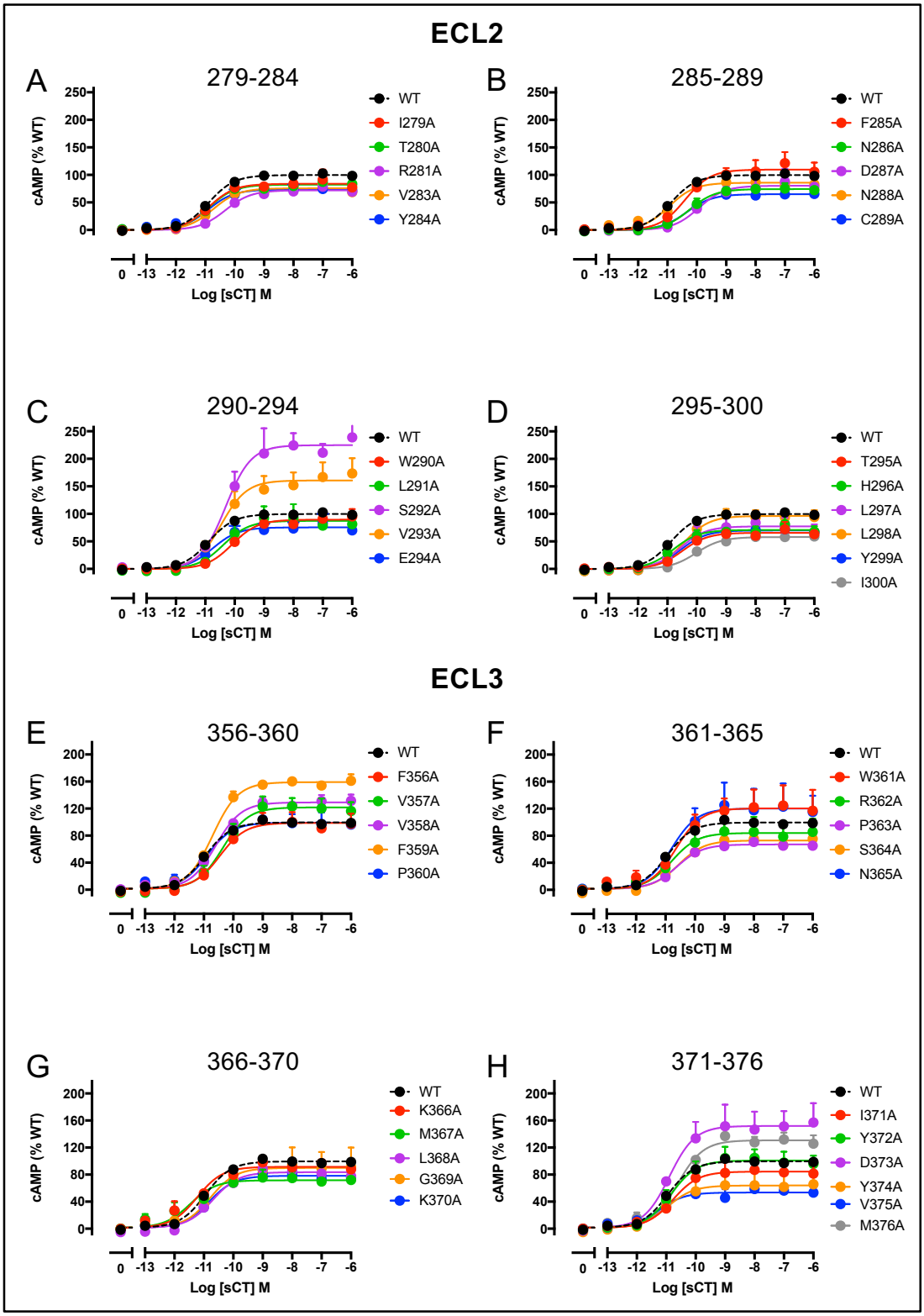

Figure S7. Concentration-response curves for sCT in cAMP accumulation assays in cells expressing the wild-type or mutant AMY_3R. **A-D.** Mutations of ECL2. **E-H.** Mutations of ECL3. Data have been normalized to the maximal response of the wild-type receptor (100%). Data have been fit with the operational model for partial agonism. The response at the wild-type receptor is shown as a dashed line. Data are mean + SEM from 3-26 independent experiments (specific "n" numbers for functional cAMP experiments are shown in Table 2).

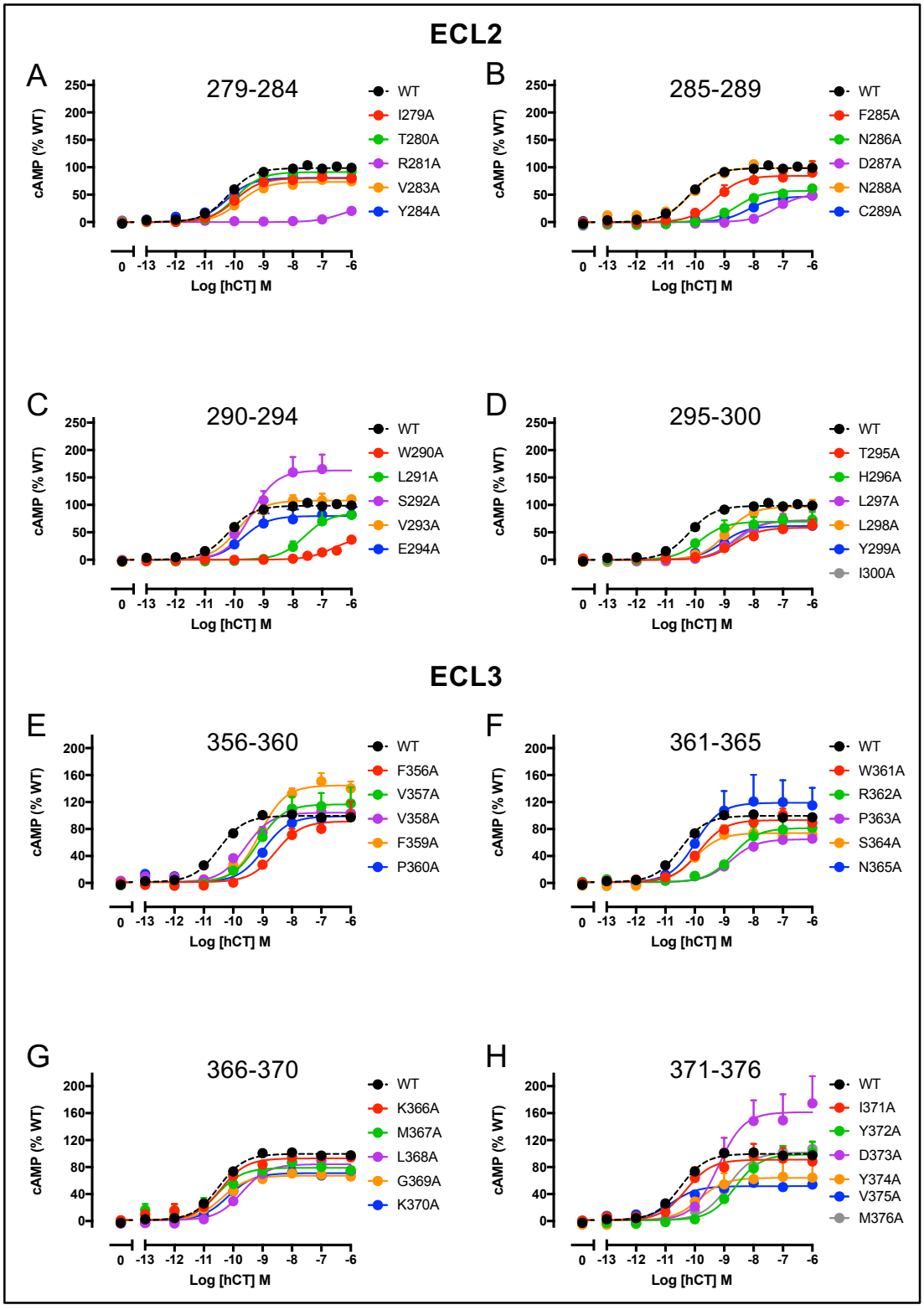

Figure S8. Concentration-response curves for hCT in cAMP accumulation assays in cells expressing the wild-type or mutant AMY_3R. **A-D.** Mutations of ECL2. **E-H.** Mutations of ECL3. Data have been normalized to the maximal response of the wild-type receptor (100%). Data have been fit with the operational model for partial agonism. The response at the wild-type receptor is shown as a dashed line. Data are mean + SEM from 3-23 independent experiments (specific "n" numbers for functional cAMP experiments are shown in Table 2).

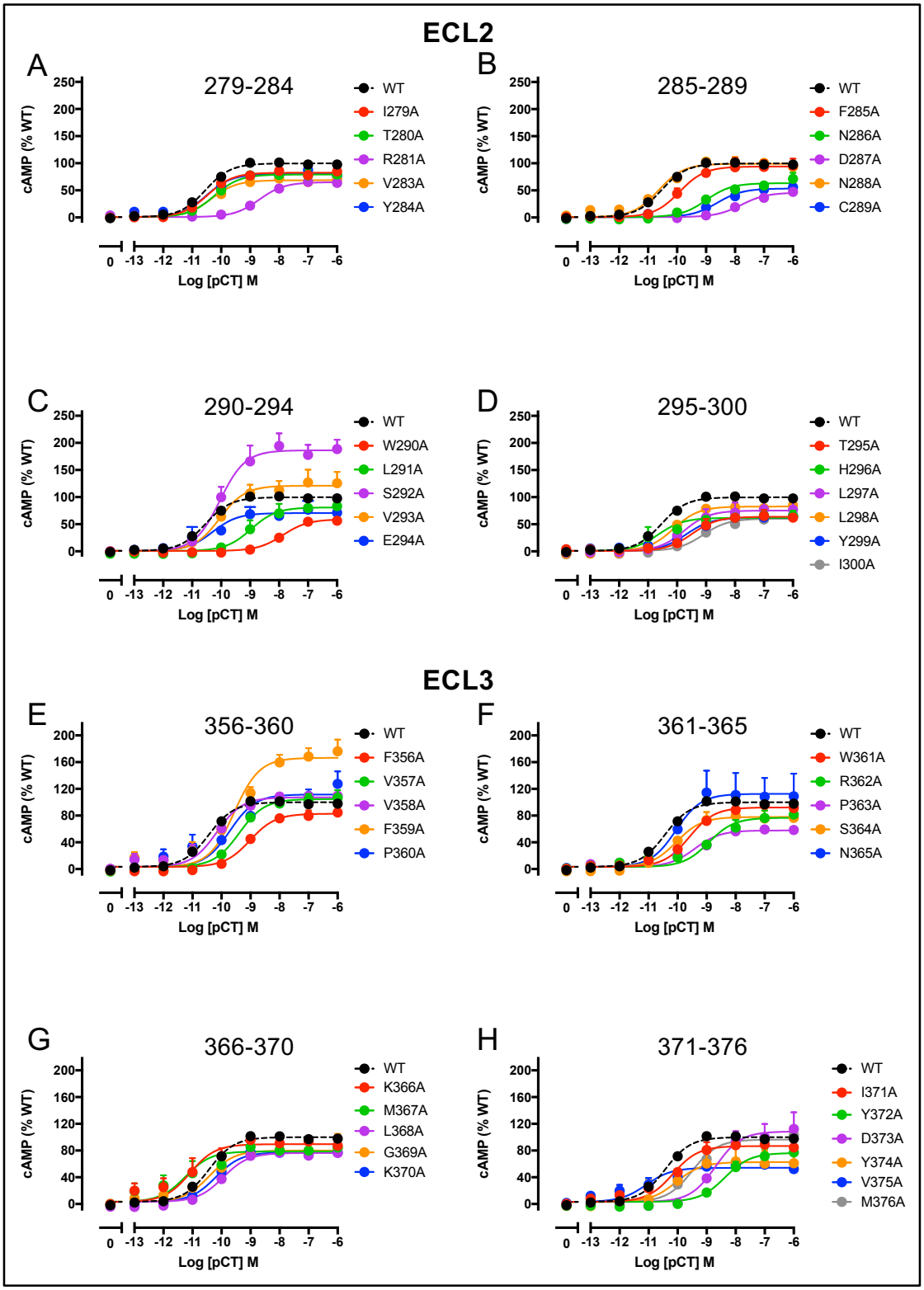

Figure S9. Concentration-response curves for pCT in cAMP accumulation assays in cells expressing the wild-type or mutant AMY_3R. **A-D.** Mutations of ECL2. **E-H.** Mutations of ECL3. Data have been normalized to the maximal response of the wild-type receptor (100%). Data have been fit with the operational model for partial agonism. The response at the wild-type receptor is shown as a dashed line. Data are mean + SEM from 3-26 independent experiments (specific "n" numbers for functional cAMP experiments are shown in Table 2).

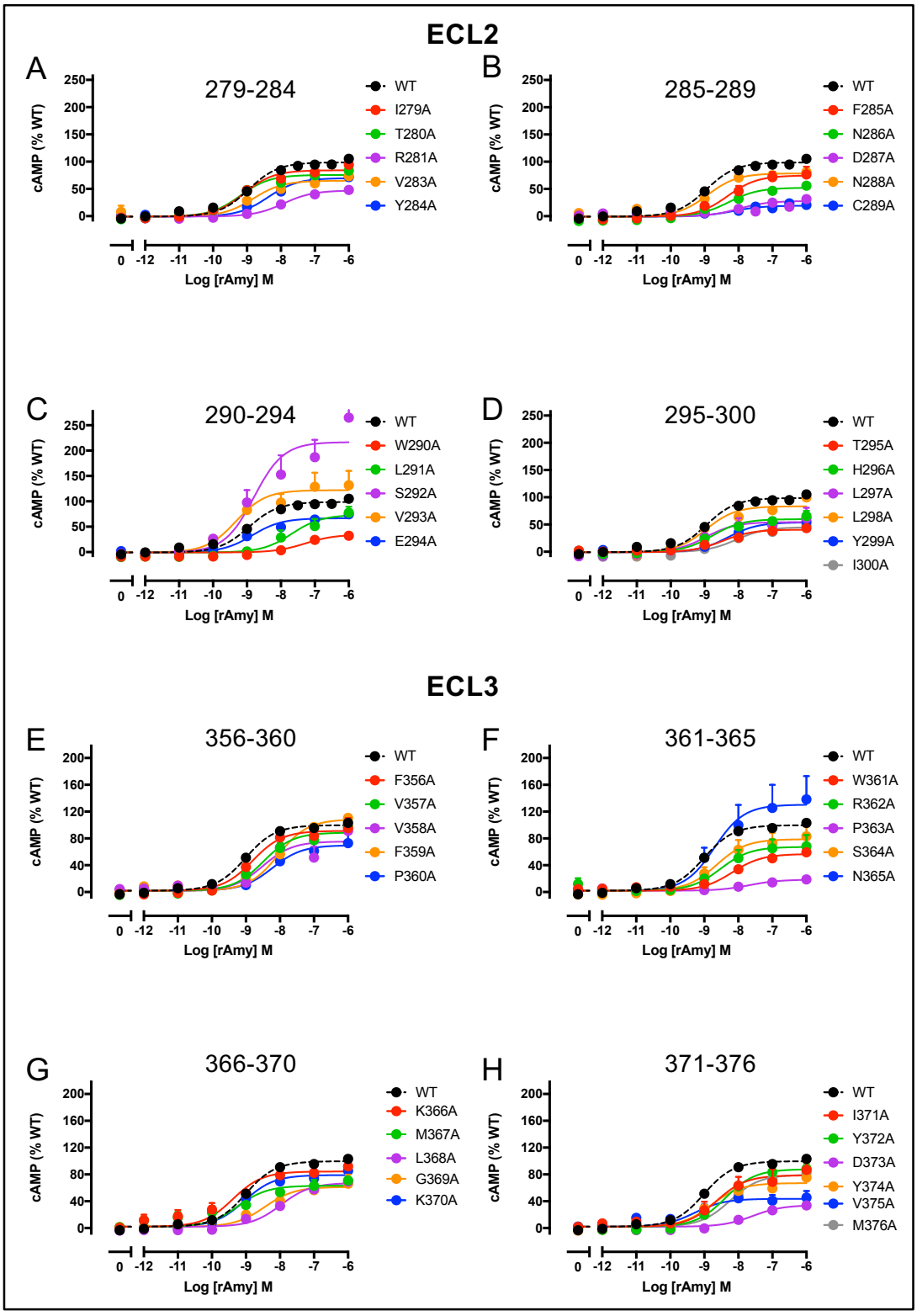

Figure S10. Concentration-response curves for rAmy in cAMP accumulation assays in cells expressing the wild-type or mutant AMY_3R. **A-D.** Mutations of ECL2. **E-H.** Mutations of ECL3. Data have been normalized to the maximal response of the wild-type receptor (100%). Data have been fit with the operational model for partial agonism. The response at the wild-type receptor is shown as a dashed line. Data are mean + SEM from 3-26 independent experiments (specific "n" numbers for functional cAMP experiments are shown in Table 2).

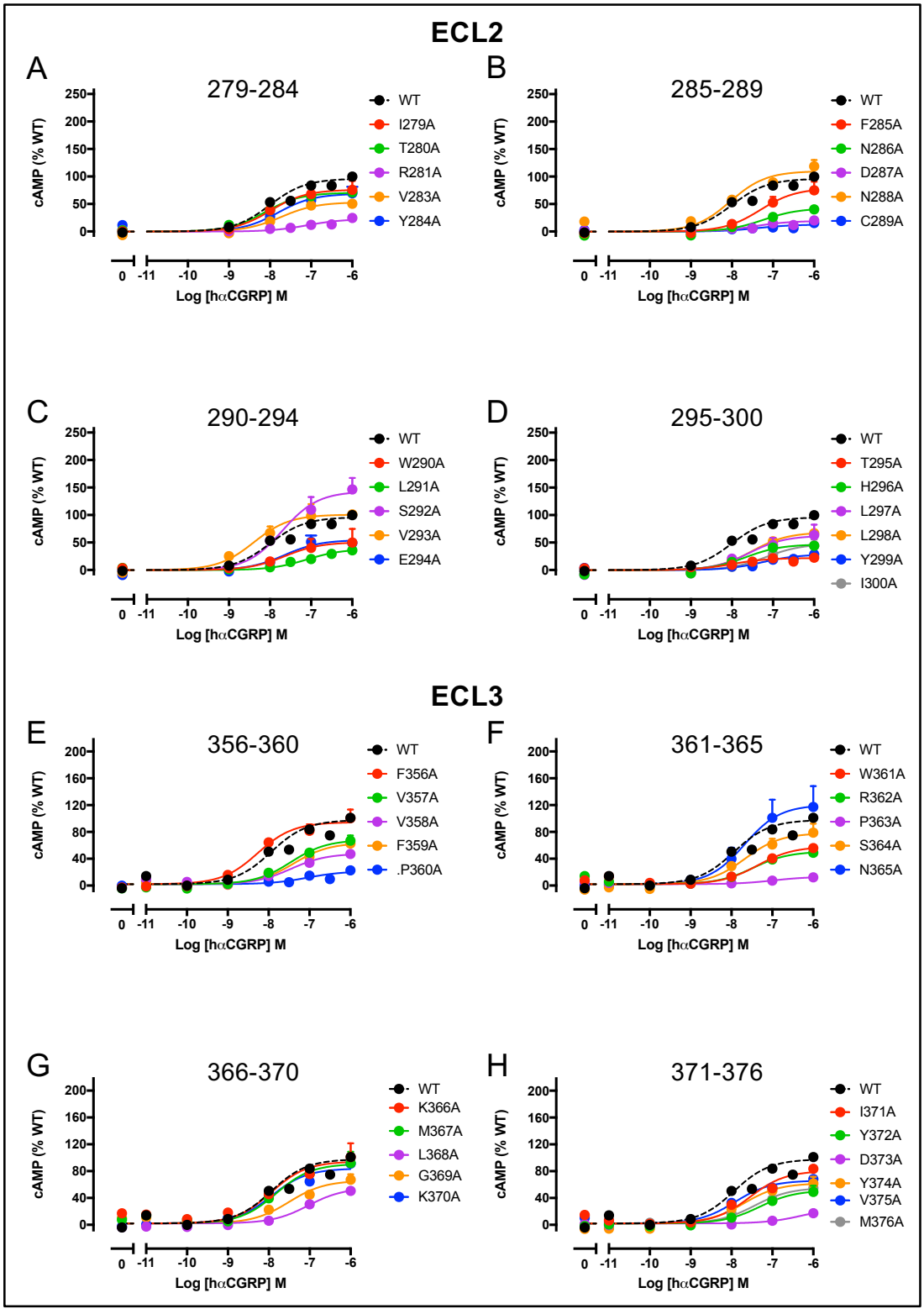

Figure S11. Concentration-response curves for hCGRP in cAMP accumulation assays in cells expressing the wild-type or mutant AMY_3R. **A-D.** Mutations of ECL2. **E-H.** Mutations of ECL3. Data have been normalized to the maximal response of the wild-type receptor (100%). Data have been fit with the operational model for partial agonism. The response at the wild-type receptor is shown as a dashed line. Data are mean + SEM from 3-34 independent experiments (specific "n" numbers for functional cAMP experiments are shown in Table 2).

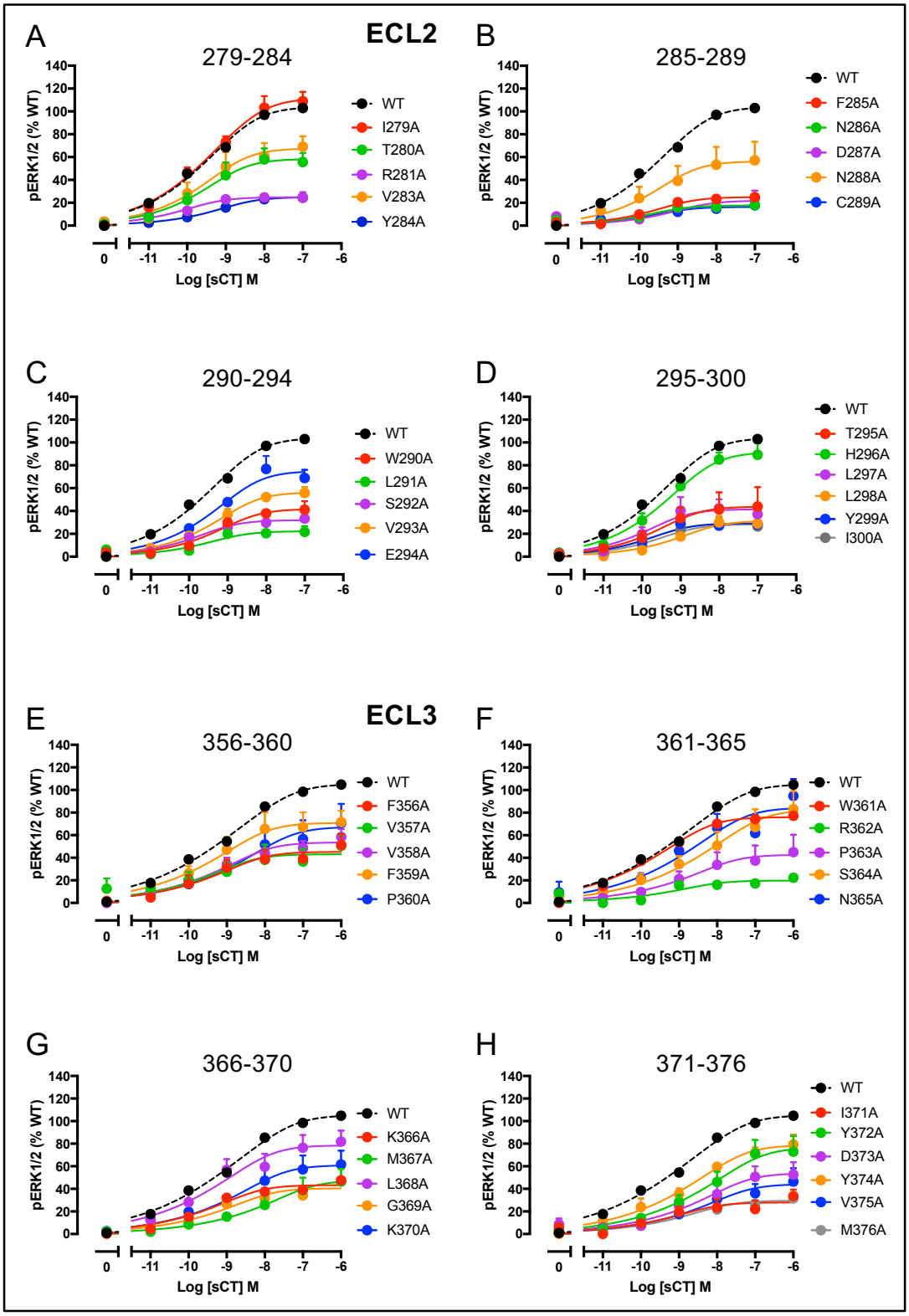

Figure S12. Concentration-response curves for sCT in ERK1/2 phosphorylation assays in cells expressing the wild-type or mutant AMY_3R. **A-D.** Mutations of ECL2. **E-H.** Mutations of ECL3. Data have been normalized to the maximal response of the wild-type receptor (100%). Data have been fit with the operational model for partial agonism. The response at the wild-type receptor is shown as a dashed line. Data are mean + SEM from 3-27 independent experiments (specific "n" numbers for functional pERK experiments are shown in Table 3).

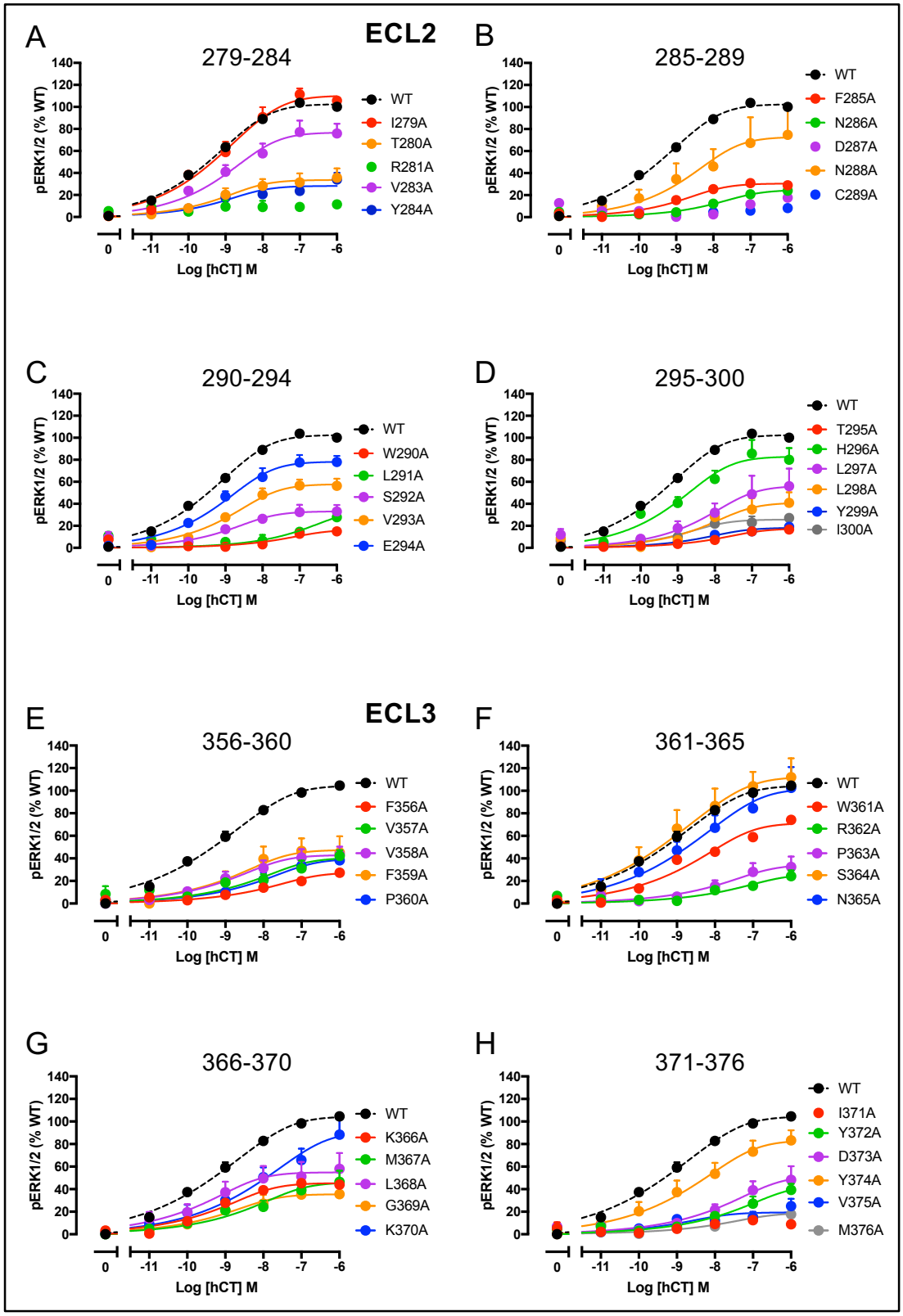

Figure S13. Concentration-response curves for hCT in ERK1/2 phosphorylation assays in cells expressing the wild-type or mutant AMY_3R. **A-D.** Mutations of ECL2. **E-H.** Mutations of ECL3. Data have been normalized to the maximal response of the wild-type receptor (100%). Data have been fit with the operational model for partial agonism. The response at the wild-type receptor is shown as a dashed line. Data are mean + SEM from 3-33 independent experiments (specific "n" numbers for functional pERK experiments are shown in Table 3).

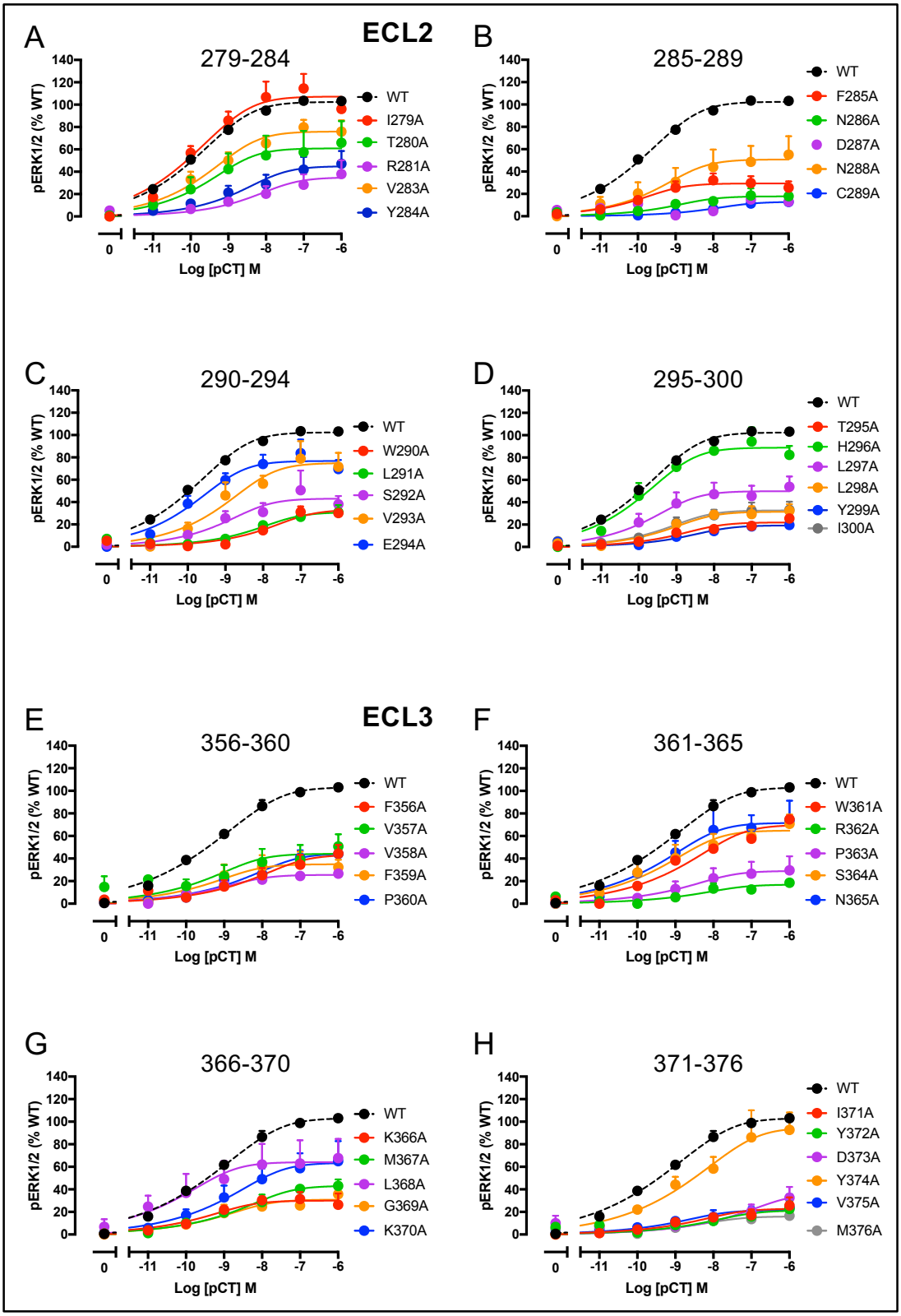

Figure S14. Concentration-response curves for pCT in ERK1/2 phosphorylation assays in cells expressing the wild-type or mutant AMY_3R. **A-D.** Mutations of ECL2. **E-H.** Mutations of ECL3. Data have been normalized to the maximal response of the wild-type receptor (100%). Data have been fit with the operational model for partial agonism. The response at the wild-type receptor is shown as a dashed line. Data are mean + SEM from 3-31 independent experiments (specific "n" numbers for functional pERK experiments are shown in Table 3).

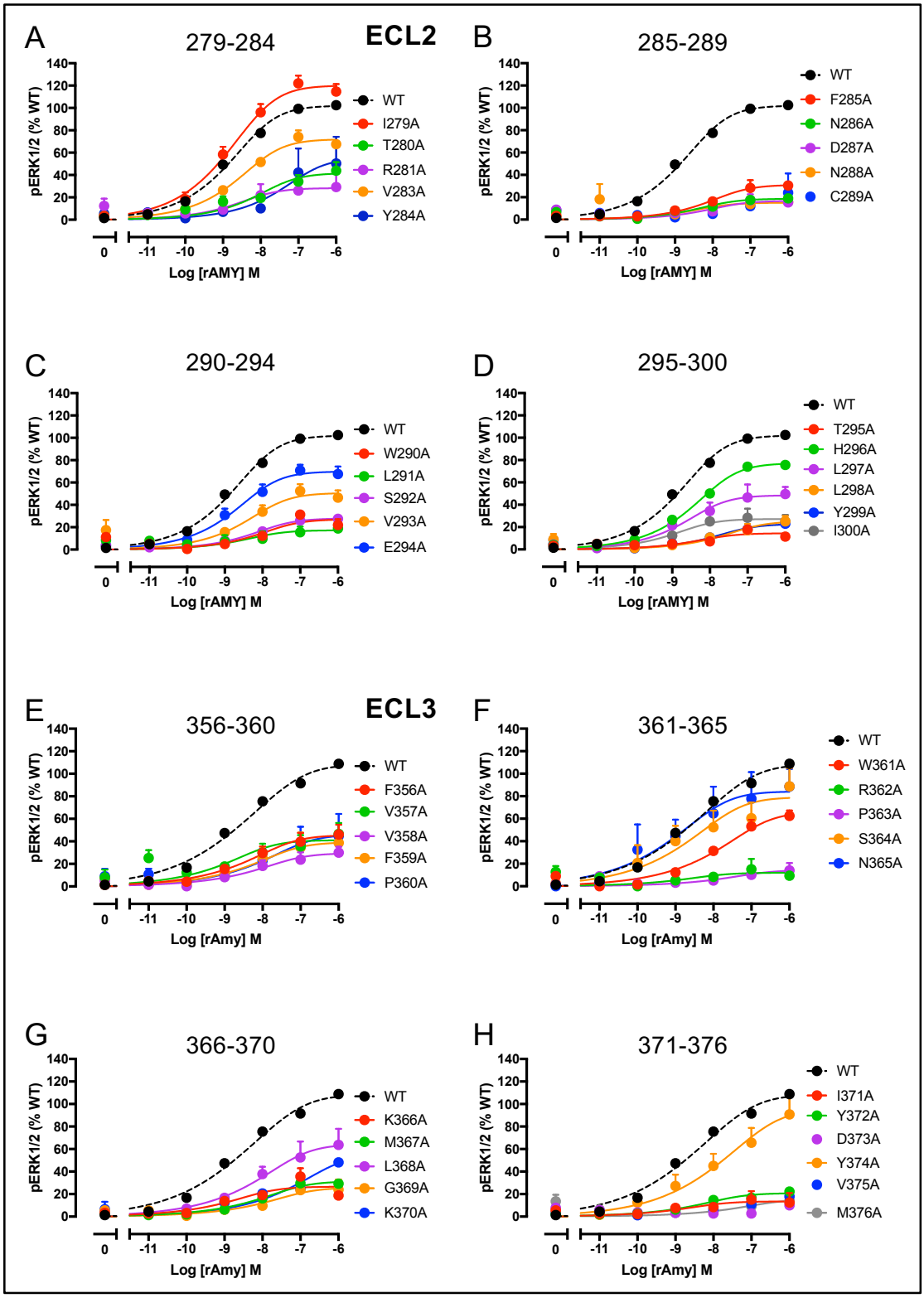

Figure S15. Concentration-response curves for rAmy in ERK1/2 phosphorylation assays in cells expressing the wild-type or mutant AMY_3R. **A-D.** Mutations of ECL2. **E-H.** Mutations of ECL3. Data have been normalized to the maximal response of the wild-type receptor (100%). Data have been fit with the operational model for partial agonism. The response at the wild-type receptor is shown as a dashed line. Data are mean + SEM from 3-33 independent experiments (specific "n" numbers for functional pERK experiments are shown in Table 3).

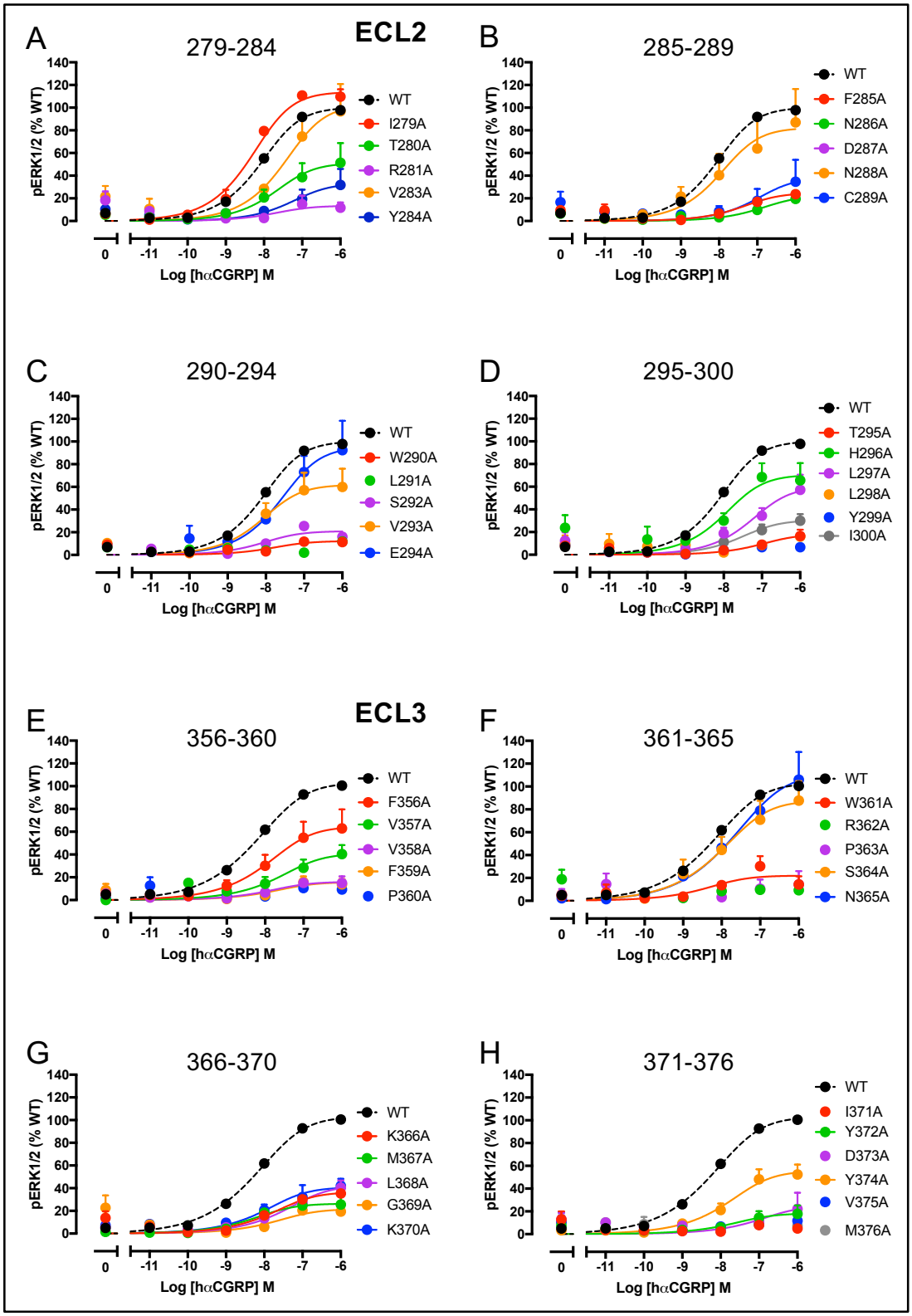

Figure S16. Concentration-response curves for hCGRP in ERK1/2 phosphorylation assays in cells expressing the wild-type or mutant AMY_3R. **A-D.** Mutations of ECL2. **E-H.** Mutations of ECL3. Data have been normalized to the maximal response of the wild-type receptor (100%). Data have been fit with the operational model for partial agonism. The response at the wild-type receptor is shown as a dashed line. Data are mean + SEM from 3-25 independent experiments (specific "n" numbers for functional pERK experiments are shown in Table 3).